

## **Thermal properties and flammability of acrylic nanocomposites based upon organophilic layered silicates**

**F. Dietsche, R. Mülhaupt\***

Institut für Makromolekulare Chemie und Freiburger Materialforschungszentrum (FMF)  
der Albert-Ludwigs-Universität Freiburg, Stefan-Meier-Strasse 21/31, D-79104 Freiburg, Germany

Received: 28 May 1999/Revised version: 24 September 1999/Accepted: 24 September 1999

### **Summary**

Thermal and mechanical properties of poly(methylmethacrylate-co-dodecylmethacrylate) nanocomposites based upon exfoliated organophilic layered silicates, were investigated as a function of the silicate and comonomer content. Layered silicates such as sodium bentonite were rendered organophilic by means of ion-exchanging sodium cations for N,N,N,N-dioctadecyl-dimethylammonium cations. Silicate exfoliation was enhanced by means of 5 and 10 wt.-% dodecylmethacrylate (LMA) addition to afford translucent reinforced acrylic nanocomposites. In contrast to conventional filled acrylic polymers, only 10 wt.-% organophilic silicate was sufficient to increase Young's modulus from 2200 to 4030 MPa, glass temperature from 72 to 80 °C and degradation temperature from 220 to 256 °C with respect to the neat MMA/LMA (90 wt.-%/10 wt.-%) copolymer. Flammability studies, performed on a cone calorimeter, revealed that the maximum heat release rate of MMA/LMA copolymer nanocomposite decreased from 837 kW/m<sup>2</sup> to 566 kW/m<sup>2</sup>. The nanocomposite morphology was examined by means of transmission electron microscopy (TEM).

### **Introduction**

An important objective in the development of engineering polymers is to reinforce the polymer matrix and to improve stiffness, strength, thermal stability and flame retardancy without sacrificing processability, optical properties, and toughness. The addition of flame retardants such as phosphorous-containing additives and special fillers can adversely affect mechanical and optical properties. Most conventional microfillers require large filler content in order to achieve matrix reinforcement at the expense of optical clarity and processability. Conventional nanofillers are rather difficult to disperse in the continuous polymer matrix due to strong interparticular interactions causing cluster formation. In an alternative approach anisotropic nanofillers are produced in-situ by means of exfoliation of organophilic layered silicates during polymerization or processing, respectively (1-5). Natural layered silicates are well known as bentonite minerals which are composed of the aluminosilicate montmorillonite where a central alumina sheet is sandwiched between two tetrahedral silica sheets. Since part of the three-valent aluminum cations are replaced by two-valent magnesium cations, the individual layers are anionically charged. This anionic charge is compensated by means of cations such as sodium located in the interlayer galleries. These intergallery sodium ions account for water swelling of such layered silicates which are rendered hydrophobic and compatible with polymers by means of ion exchange of sodium cations for alkylammonium cations. When adequate compatibility between polymer matrix and organophilic layered silicates is achieved, shear forces during polymerization or polymer processing are sufficient to disperse individual layers or multiple layer assemblies as nanoparticles in the polymer matrix. This

---

\* Corresponding author  
e-mail: mulhaupt@mf.uni-freiburg.de

process is known as exfoliation. In comparison to conventionally filled polymers, nanocomposites exhibit high stiffness, higher heat distortion temperature and thermal stability, and much lower gas and fluid permeability at low filler content which are typically < 10 wt.-% (5). Recently, Gilman and Giannelis reported improved flame retardancy of polypropylene, polystyrene, polyamide and epoxy nanocomposites, as evident from 40 to 60% lower heat release rates during combustion (6). The nanocomposite appeared to promote formation of char layers which act as an insulator and mass transfer barrier.

In pioneering advances by Ciardelli, Ruggeri and coworkers (7,8), polymethylmethacrylate (PMMA) nanocomposites were obtained using functionalization of montmorillonite by means of methyl methacrylate copolymers containing ammonium cations in the side chain. Such copolymers were added separately or produced in-situ using montmorillonite, modified by means of ion exchange with various N,N,N,N-trialkylammonium-ethylacrylates. Also emulsion polymerization of MMA in the presence of sodium montmorillonite has been introduced to produce acrylic nanocomposites (9,10,15,16). In our research, exfoliation of layered silicates, which were rendered organophilic by means of ion exchange with N,N,N,N-dioctadecyl-dimethyl-ammonium chloride, was achieved when dodecylmethacrylate (LMA) was added during free radical bulk polymerization. Such acrylic nanocomposites were observed to prevent formation of dripping burning droplets of burning polymer (5). Here we report the investigation of thermal and mechanical properties as well as flammability behavior, measured by means of cone calorimetry, as a function of silicate and LMA content.

## Experimental

### *Materials*

Organophilic bentonite, modified dioctadecyldimethyl ammonium ions, (0,16 g modifier/g filler) with particle sizes of 1 - 5  $\mu\text{m}$  and density of 1,8  $\text{g}/\text{cm}^3$  was supplied by Süd-Chemie AG / Moosburg, Germany. Methylmethacrylate was obtained from Röhm AG / Darmstadt, Germany, and used without further purification. Polymerizations were initiated by 0,1 wt.-% azoisobutyronitril (AIBN) from Fluka at 70 °C.

### *Preparation of bentonite intercalated PMMA/LMA-copolymer*

Sodium bentonite, ion-exchanged with N,N,N,N-dioctadecyldimethyl ammonium chloride, was suspended in the amount of LMA, required to afford the MMA/LMA/bentonite ratios listed in Table 1. Swelling was performed for the duration of 1 hour at room temperature. The resulting highly viscous paste was diluted with MMA and sonicated for the duration of 30 min using a Bandalin RK 52 sonicator equipped with a water bath. Under argon atmosphere this mixture was transferred into a mold to produce sheets of 2 or 4 mm thickness. Polymerizations were carried out at 70 °C using AIBN as initiator (0,1 wt.-% with respect to monomer). Polymerization was performed in bulk at 70 °C for 5 h. The reaction was monitored via heat evolution. Residual MMA was removed by heating to 100 °C for 12 h in oil pump vacuum. High conversion of MMA and LMA was monitored by the disappearance of characteristic monomer  $^1\text{H-NMR}$ -vinyl signals at 4,6 and 6,3 ppm.

### *Characterization of nanocomposites*

Mechanical properties were measured on samples (60x12x4 mm) by means of stress/strain testing according to DIN 53455 using a Zwick 4202 tensile tester and crosshead speed of 1 mm/min. At

least 7 samples were measured to assure reproducibility. The fracture toughness  $K_{Ic}$  was determined by tensile experiments on compact tension (CT) specimen in a Zwick tensile testing machine at a crosshead speed as slow as 0,18 mm/min. The dimensions of the CT-specimens were thickness  $B = 4$  mm, height  $H = 8$  mm, effective width  $W = 8$  mm. The effective crack length  $a$  was determined by measuring in a travelling microscope after the tensile test. The maximum load measured in the experiment was taken to calculate  $K_{Ic}$  according to Eq.1.

$$(Eq.1) \quad K_{Ic} = \frac{P_c * (2W + a)}{(B * (W - a))^{1.5}} * Y\left(\frac{a}{W}, \frac{H}{W}\right)$$

The geometrical factor  $Y\left(\frac{a}{W}, \frac{H}{W}\right)$  valid for compact tension specimens was calculated according to Srawley and Gross (11).

#### *Wide-angle X-ray scattering (WAXS)*

The degree of swelling and the interlayer distance were studied by means of wide angle X-ray scattering (WAXS), using an image-plate-system with the  $CuK\alpha$  radiation ( $\lambda = 1,5418$  nm) and a scanning time of 500 s.

#### *Thermal analysis*

Thermogravimetric (TGA) investigations were recorded on a Netzsch simultaneous thermoanalyser (STA 409), controlled by a Netzsch TASC 412/2 unit, in the presence of air (flow: 150 ml/min), using a heating rate of 5 °C/min. Evaluations of flammability were done using the cone calorimeter. The tests were done at an incident heat flux of 35 kW/m<sup>2</sup> using the cone heater. A flux of 35 kW/m<sup>2</sup> represents a typical small-fire scenario. Peak heat release rate (hrr) and specific extinction area (sea) data, measured at 35 kW/m<sup>2</sup>, are reproducible to within 241 ± 8%. The cone data reported here is the average of two or three replicated experiments. Flammability properties were measured on cone samples (100x100x8 mm).

#### *Morphological analysis (TEM)*

The morphology of the samples was examined by means of transmission electron microscopy (TEM) using a Zeiss EM 902 and 80 keV acceleration voltage. Ultrathin specimen of 30 - 50 nm were cut at room temperature using an ultramicrotome (Ultracut E, Reichert & Jung) equipped with a diamond knife. Ultrathin sections were analyzed without staining.

## **Results and discussions**

Sodium bentonite was rendered organophilic by means of ion exchange with N,N,N,N-dioctadecyl-dimethyl-ammonium cations and added during copolymerization of MMA containing 5 and 10 wt.-% dodecylmethacrylate (LMA) as compatibilizer in order to enhance hydrophobic interactions between acrylic polymer matrix and organophilic silicate layers. Preferably, the organophilic bentonite was swollen with LMA prior to MMA addition. The properties of the nanocomposites containing 5 wt.-% (NC5) and 10 wt.-% LMA (NC10) as well as 2, 5, and 10 wt.-% organophilic silicate (NC/2, NC/5, NC/10) are listed in Table 1. Superstructure formation of the resulting acrylic nanocomposites were examined by means of wide angle X-ray scattering (WAXS) which confirmed effective exfoliation of the silicate layers when LMA was present. The WAXS traces are displayed in Figure 1. The interlayer spacing increased from 0,9 nm for sodium bentonite to 2,1 nm

for organophilic bentonite after ion exchanging sodium cations for N,N,N,N-dioctadecyl-dimethylammonium cations. Upon addition of LMA (50 wt.-% with respect to organophilic bentonite), swelling was accompanied by increasing interlayer distance to 5,2 nm. Formation of the nanocomposite containing 10 wt.-% LMA and 5 wt.-% organophilic silicate accounted for exfoliation with interlayer distance  $> 7$  nm (cf. Trace C, Fig.1)

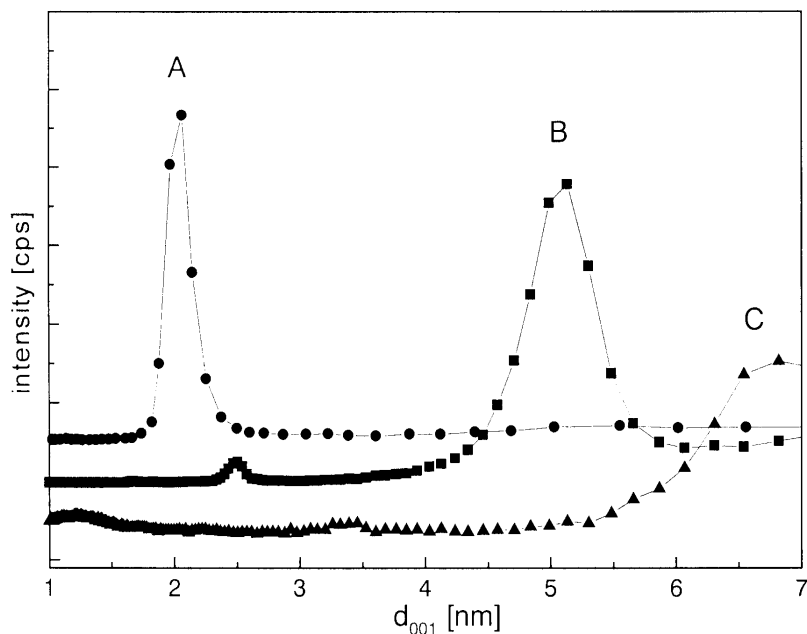


**Figure 1** WAXS traces of organophilic bentonite (A); organophilic bentonite / LMA (50 wt.-%/50 wt.-%) mixture (B); nanocomposite NC10/5 (C).

In addition to WAXS, nanocomposite superstructures were imaged by means of transmission electron microscopy (TEM). Figure 2 displays the TEM image of MMA/LMA (90/10) containing 5 wt.-% organophilic layered silicate (nanocomposite NC10/5) before flammability testing. The dark lines correspond to individual silicate layers of 1 - 5 nm thickness and 80 - 900 nm length which separated by about  $> 7$  nm. This confirms effective exfoliation. The interlayer distance is in agreement with that determined by means of WAXS.

Poly(MMA-co-LMA) nanocomposites exhibited rather unusual thermal and mechanical properties. Since LMA incorporation introduced an internal plasticizer, the resulting copolymers had lower glass temperature and Young's modulus with respect to PMMA. Both stiffness and glass temperature decreased with increasing LMA content. However, it is apparent from Table 1 that addition of organophilic bentonite to MMA/LMA increased both stiffness and glass transition temperature with respect to the corresponding copolymer. Most likely LMA, which was added prior to MMA addition, was polymerized preferably at the silicate interface, thus preventing plastification of the PMMA matrix. While all nanocomposites were rather soft at LMA content exceeding 5 wt.-%, LMA contents of  $< 5$  wt.-% accounted for substantial improvements in toughness without sacrificing stiffness. At 10 wt.-% content of organophilic silicate Young's modulus increased from 2200 to 4030 MPa.

Polymer combustions involves a rather complex series of stages with the first one being associated with pyrolysis of the acrylic polymer to yield volatile decomposition products, i.e., mainly monomers (12,13). These volatiles will then continue to burn by the chain propagation process involving reactions of free radicals.

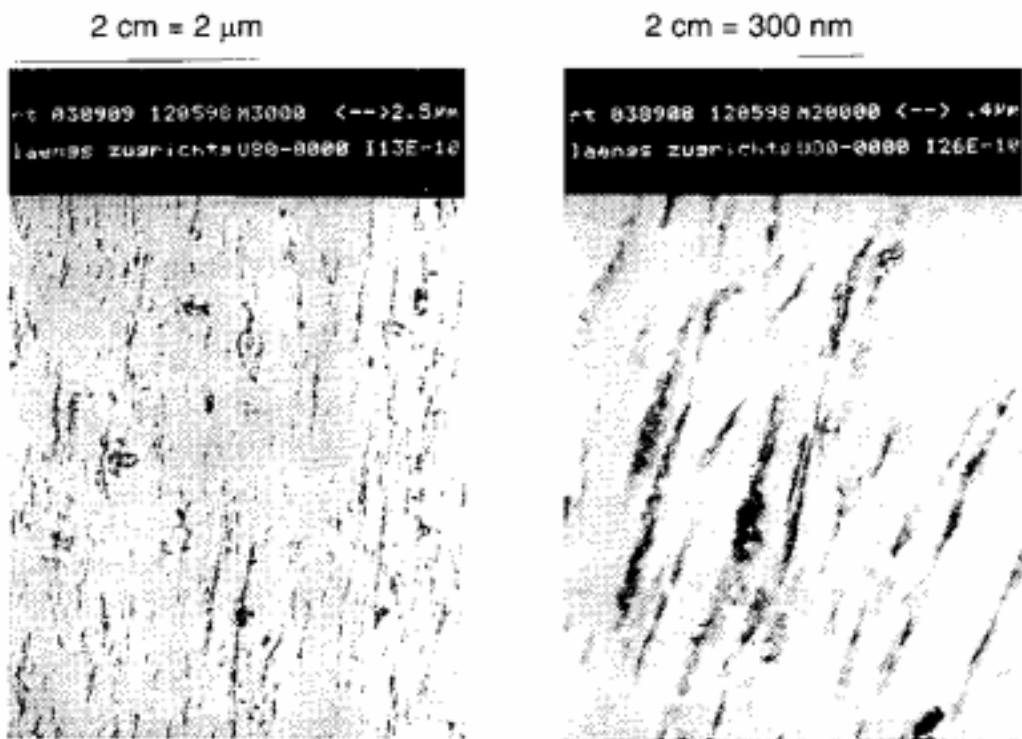


**Figure 2** TEM of a section of the nanocomposite NC10/5 showing exfoliated silicate layers which are likely to function as insulator and diffusion barrier.

**Table 1:** Thermal and mechanical properties of poly(MMA-co-LMA) containing 5 (P5) and 10 wt.-% LMA (P10) and corresponding nanocomposites (NC)

copolymer/ nanocomposite	LMA (wt.-%)	silicate (wt.-%)	T <sub>g</sub> (°C) <sup>a</sup>	Young's modulus (MPa)	K <sub>1c</sub>	max. HRR (kW/m <sup>2</sup> )	d <sub>501</sub> (nm)	TGA (5 % wt.) <sup>b</sup> (°C)
PMMA	0	0	110	3300	0,98	827 <sup>12</sup>	-	219
P5	5	0	85	2500	1,44	877	-	218
NC5/5	5	5	90	4370	0,95	745	>5,4	224
P10	10	0	72	2200	1,88	837	-	220
NC10/2	10	2	75	3620	1,34	752	>7,1	235
NC10/5	10	5	76	3890	1,23	745	>6,8	239
NC10/10	10	10	80	4030	0,89	566	>5,1	256

<sup>a</sup> determined by dynamic mechanical analysis at a heating rate of 5 °C/min

<sup>b</sup> thermogravimetric analysis under air; temperature at which 5 wt.-% weight loss was observed

Flammability studies of acrylic nanocomposites and the corresponding polymers were performed by means of a cone calorimeter. As apparent from Figures 3 and 4, both maximum and average heat release rate (hrr) were significantly lowered in the case of exfoliated acrylic nanocomposites, even at low content of organophilic layered silicate which was varied between 2 and 12 wt.-%.

The primary difference between the flammability behaviour of neat acrylic copolymers and their corresponding nanocomposites relates to the maximum and the average heat release rate. The specific extinction area (sea), a measure of fume-density, and the duration of combustion increased

with silicate mass fraction. Bulk copolymers burned with a heat flux of  $35 \text{ kW/m}^2$  for the duration of 250 s, in contrast to the corresponding nanocomposites with much longer burning times of 270 - 345 s (NC10/2-12). The maximum rate of heat release decreased from 877 to  $566 \text{ kW/m}^2$  for NC10/12. In comparison, the average heat release rate decreased from  $512 \text{ kW/m}^2$  for P10 to  $372 \text{ kW/m}^2$  for the corresponding nanocomposite. The specific extinction area (sea) increased from 136 for P10 to  $157 \text{ m}^2/\text{kg}$  for NC10/12.

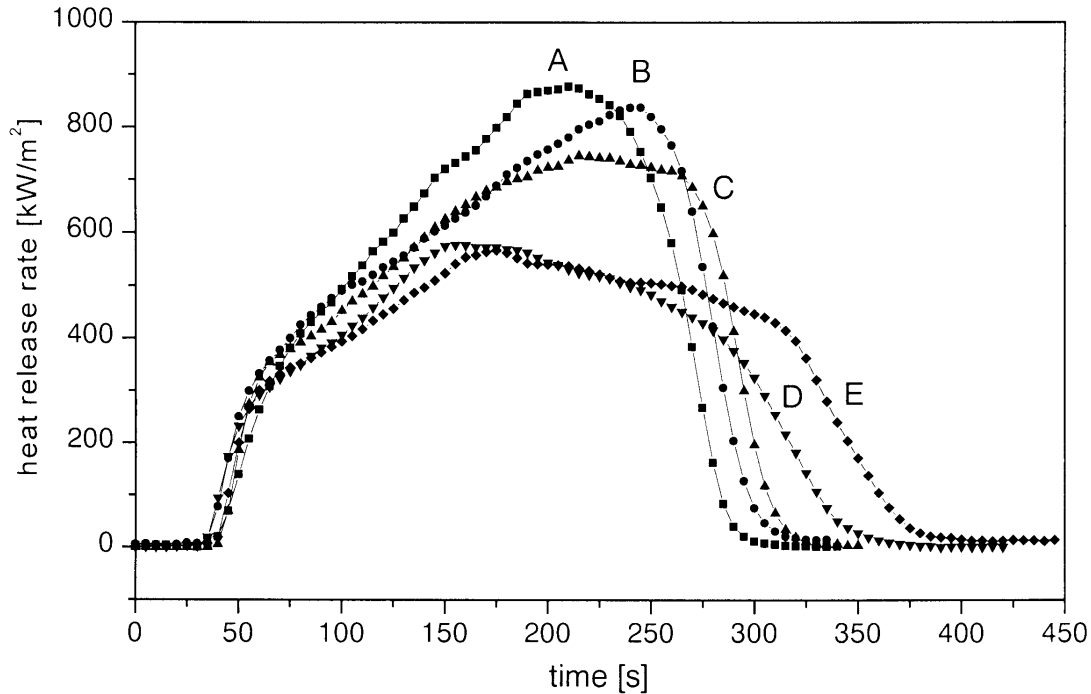


**Figure 3** Comparison of the heat release rate (hrr) plot for copolymer (A) and acrylic nanocomposites (B-E) at  $35 \text{ kW/m}^2$  heat flux, showing a 34 % reduction in hrr for the nanocomposite NC10/10.

Visual examination of the pyrolysis revealed that after 30 s, when the mass loss rate for the nanocomposite slowed down with respect to that of the neat copolymer, the surface of the nanocomposite was completely covered by char. Comparison of the residue yields for copolymers and nanocomposites indicated much higher char yields for nanocomposites. These observations are in accord with earlier observations by other groups (6).

A multilayered silicate structure displayed in Figure 2 was imaged by means of TEM before combustion. Obviously, the darker, 1 - 5 nm thick, silicate sheets formed a fairly large array during combustion. This multilayer silicate array may serve as excellent insulator and mass transport barrier, thus slowing down the diffusion of volatile decomposition products generated during decomposition of the acrylic polymer. According to thermogravimetric analysis (TGA) nanocomposite formation improved thermal stability, as measured by the temperature at which 5 wt.-% weight loss was observed. Typical TGA traces are displayed in Figure 5 for the MMA/LMA (90/10) copolymer and the corresponding nanocomposites containing 2 (NC10/2) and 10 wt.-% organophilic layered silicate (NC10/10). In the case of the nanocomposite NC10/10 degradation temperature in air was  $256 \text{ }^\circ\text{C}$  with respect to only  $218 - 220 \text{ }^\circ\text{C}$  for the corresponding copolymer in the absence of organophilic silicate.

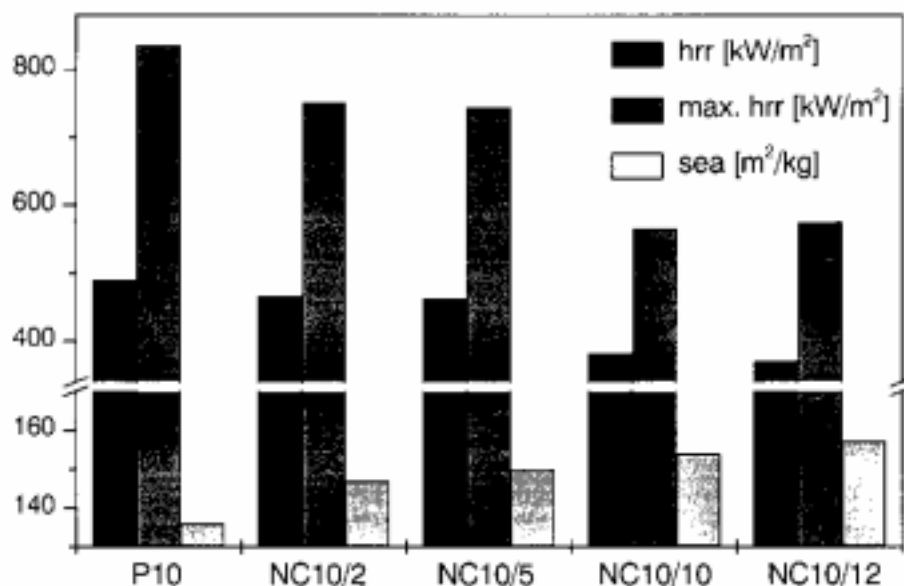


**Figure 4** Comparison of the heat release rate (hrr), the maximum heat release rate (max. hrr) and the specific extinction area (sea) for acrylic copolymer and nanocomposites

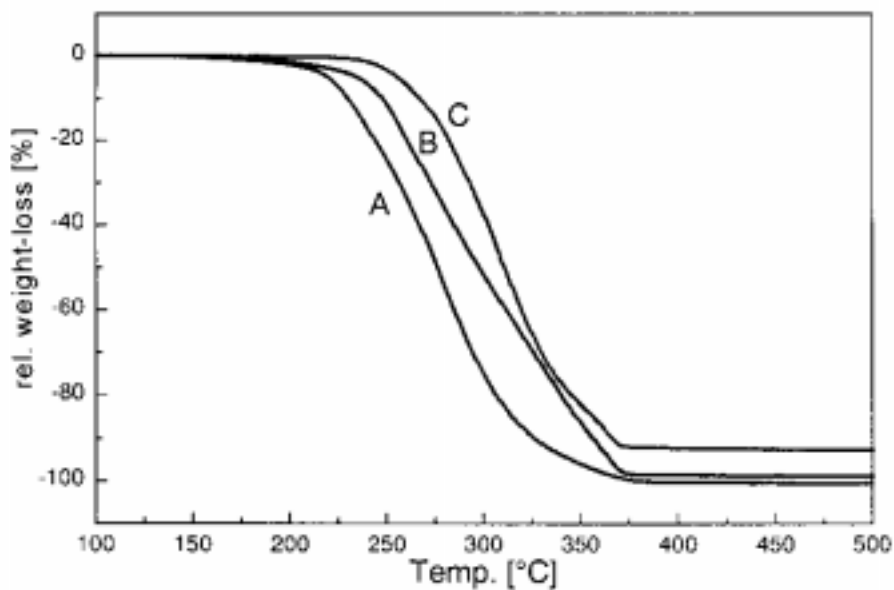


**Figure 5** Comparison of the degradation temperature (5 wt.-% weight loss) measured by thermogravimetry under air-atmosphere for MMA/LMA (90/10) (A) and the corresponding nanocomposites NC10/2 (B); NC10/10 (C).

## Conclusions

The formation of nanocomposites containing exfoliated compatibilized organophilic silicate layers with high aspect ratio (~100 - 150) represents an attractive route to polymeric materials with

unique property combinations. Compatibility between acrylic matrix and silicate layers, rendered organophilic by means of ion exchange with dioctadecyl-dimethyl-ammonium cations, can be achieved via hydrophobic interactions involving dodecyl methacrylate (LMA) units incorporated in the PMMA backbone. Only in the presence of LMA comonomer, translucent acrylic nanocomposites with nanometer-scaled anisotropic silicate layered are formed. Less than 10 wt.-% organophilic silicates are sufficient to improve stiffness, glass temperature, thermal stability and flame retardancy with respect to the corresponding copolymers as well as PMMA. In contrast to most conventional fillers and solid flame retardants, better performance is achieved without sacrificing impact strength and processability. Key features of nanocomposites in combustion are significantly reduced average heat release rate and enhanced char formation. Most likely, the silicate nanolayers reduce diffusion and assemble to char layers which function as diffusion barriers and effective thermal insulators. The combination of nanocomposite formation with flame retardant additives is likely to lead to the development of new polymeric materials with simultaneous improvement of mechanical and barrier properties as well as fire retardancy.

### Acknowledgements

The authors thank the Deutsche Forschungsgemeinschaft (DFG) for their support as part of the Sonderforschungsbereich SFB 428 (Strukturierte Makromolekulare Netzwerksysteme). We would also thank Prof. Dr. S. J. Grayson for cone calorimeter analysis by fire-testing-technology (FTT).

### References

1. Lagaly G (1986) in Wilson AD, Posser HT (eds.) Development in Ionic Polymers. Applied Science Publishers, London, Chapter 2: 77
2. Akelah A (1995) in Prasad N, Mark JE, Fai TJ (eds.) Polymers and Other Advanced Materials. Plenum Press, New York, 625
3. Giannelis EP (1996) Adv Mater 8: 29
4. Pinnavaia TJ (1996) in Lan T, Wang Z, Shi H, Kaviratna PD in Chow GM, Gonsalves KE (eds.) Nanotechnology, Washington, ACS Symposium Ser 622: 251
5. Zilg C, Reichert P, Dietsche F, Engelhardt T, M??lhaupt R (1998) Kunststoffe 88: 1812
6. Gilman JW, Kashiwagi T, Brown JET, Lomakin S, Giannelis EP, Manias E (1998) 43rd SAMPE Symp Exhib (Materials and Process Affordability - Key to the Future) 4: 1053
7. Biasci L, Aglietto M, Ruggeri G, Ciardelli F (1994) Polymer 35: 3296
8. Forte C, Geppi M, Giamberini S, Ruggeri G, Veracini CA, Mendez B (1998) Polymer 39: 2651
9. Bhattacharya J, Chakravarti SK, Talapatra S (1989) J Poly Sci Poly Chem 27: 3977
10. Lee DC, Jang LW (1996) J Appl Poly Sci 61: 1117
11. Srawley JE, Gross L (1972) Eng Fr Mech 4: 587
12. Babrauskas V, Grayson SJ (1992) Heat Release in Fires. Elsevier Applied Science, London New York
13. Troitzsch J (1982) Brandverhalten von Kunststoffen, Hanser Verlag, Munich vol 16: 590
14. Brown RP (1984) Kunststoff-Prüftechnik, Hanser Verlag, Munich, vol 14: 485
15. Blumstein A (1965) J Polym Sci Poly Chem 3:2653
16. Blumstein A(1965) J Polym Sci Poly Chem 3:2665